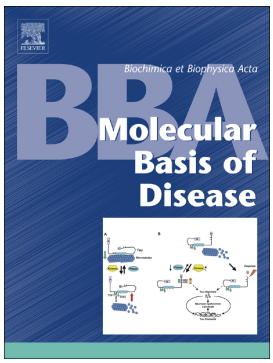

Mechanisms of canalicular transporter endocytosis in the cholestatic rat liver

Gisel S. Miszczuk, Ismael R. Barosso, María Cecilia Larocca, Julieta Marrone, Raúl A. Marinelli, Andrea C. Boaglio, Enrique J. Sánchez Pozzi, Marcelo G. Roma, Fernando A. Crocenzi

PII: S0925-4439(18)30016-4
DOI: https://doi.org/10.1016/j.bbadis.2018.01.015
Reference: BBADIS 65031

To appear in:

Received date: 25 September 2017
Revised date: 12 January 2018
Accepted date: 16 January 2018

Please cite this article as: Gisel S. Miszczuk, Ismael R. Barosso, María Cecilia Larocca, Julieta Marrone, Raúl A. Marinelli, Andrea C. Boaglio, Enrique J. Sánchez Pozzi, Marcelo G. Roma, Fernando A. Crocenzi , Mechanisms of canalicular transporter endocytosis in the cholestatic rat liver. The address for the corresponding author was captured as affiliation for all authors. Please check if appropriate. Bbadis(2018), https://doi.org/10.1016/j.bbadis.2018.01.015

MECHANISMS OF CANALICULAR TRANSPORTER ENDOCYTOSIS IN THE CHOLESTATIC RAT LIVER

Gisel S. Miszczuk[1], Ismael R. Barosso[1], María Cecilia Larocca[1], Julieta Marrone[1], Raúl A. Marinelli[1], Andrea C. Boaglio[1], Enrique J. Sánchez Pozzi[1], Marcelo G. Roma[1], and Fernando A. Crocenzi[1]

[1]Instituto de Fisiología Experimental (IFISE) – Consejo Nacional de Investigaciones Científicas y Técnicas (CONICET).
Facultad de Ciencias Bioquímicas y Farmacéuticas – Universidad Nacional de Rosario
Suipacha 570, S2002LRL, Rosario
ARGENTINA

Correspondence to:

Fernando A. Crocenzi, PhD
Instituto de Fisiología Experimental, Facultad de Ciencias Bioquíımicas y Farmacéuticas
Universidad Nacional de Rosario
Suipacha 570, S2002LRL, Rosario, Santa Fe, Argentina
E-mail: crocenzi@ifise-conicet.gov.ar or fcrocen@unr.edu.ar
Phone: +54-341-4305799

Conflicts of interest: none

Author´s contribution: Conception and design of the study (FAC, MGR, RAM), data collection (GSM, IRB, JM, ACB), data analysis and interpretation (GSM, MCL, EJSP), writing of the manuscript (FAC, GSM, MGR), critical revision of the paper (RAM, EJSP).

ABSTRACT

Impaired canalicular secretion due to increased endocytosis and intracellular retention of canalicular transporters such as BSEP and MRP2 is a main, common pathomechanism of cholestasis. Nevertheless, the mechanisms governing this process are unknown. We characterized this process in estradiol 17 β-D-glucuronide (E17G)-induced cholestasis, an experimental model which partially mimics pregnancy-induced cholestasis. Inhibition of clathrin-mediated endocytosis (CME) with monodansylcadaverine (MDC) or K^+ depletion, but not the caveolin-mediated endocytosis inhibitors filipin and genistein, prevented E17G-induced endocytosis of BSEP and MRP2, and the associated impairment of activity of these transporters in isolated rat hepatocyte couplets (IRHC). Immunofluorescence and confocal microscopy studies showed that, in E17G-treated IRHC, there was a significant increase in the colocalization of MRP2 with clathrin, AP2, and Rab5, three essential members of the CME machinery. Knockdown of AP2 by siRNA in sandwich-cultured rat hepatocytes completely prevented E17G-induced endocytosis of BSEP and MRP2. MDC significantly prevented this endocytosis, and the impairment of bile flow and biliary secretion of BSEP and MRP2 substrates, in isolated and perfused livers. BSEP and MRP2, which were mostly present in raft (caveolin-enriched) microdomains in control rats, were largely found in non-raft (clathrin-enriched) microdomains in livers from E17G-treated animals, from where they can be readily recruited for CME. In conclusion, our findings show that CME is the mechanism responsible for the internalization of the canalicular transporters BSEP and MRP2 in E17G-induced cholestasis. The shift of these transporters from raft to non-raft microdomains could be a prerequisite for the transporters to be endocytosed under cholestatic conditions.

Keywords: canalicular transporters; clathrin-mediated endocytosis; estrogen-induced cholestasis; lipid rafts.

Abbreviations: BS, bile salts; BSEP, bile salt export pump; MRP2, multidrug resistance-associated protein 2; E17G, estradiol 17 β-D-glucuronide; EE, 17α-ethynylestadiol; IRHC, isolated rat hepatocyte couplets; CME, clathrin mediated endocytosis; MDC, monodansylcadaverine; siRNA, small interfering RNA; SCRH, sandwich cultured rat hepatocytes; IPL, isolated and perfused livers; TC, taurocholate; DNP-SG, dinitrophenyl glutathione; cVA, canalicular vacuolar accumulation; CGamF, cholyl-glycylamidofluorescein; GS-MF, glutathione methylfluorescein.

1. INTRODUCTION

Bile formation is an osmotic-driven process that involves the concentrative canalicular excretion of osmotically active biliary solutes, such as bile salts (BS) and glutathione. Therefore, two of the most relevant canalicular transporters involved in bile formation are the BS export pump (BSEP) which transports monoanionic BS, and multidrug resistance-associated protein 2 (MRP2) which transports glutathione and glutathione conjugates, besides a wide variety of anionic compounds.

Under physiological conditions, canalicular transporters undergoes constitutive internalization to a subapical vesicular compartment, which constitute a reservoir of transporters available for targeting to the apical domain on demand [1]. It has been demonstrated that constitutive endocytosis of BSEP is mediated by clathrin-coated vesicles; a conserved sequence in its C-terminal domain, which is characteristic to all ABC transporters, is indispensable for this process [2]. Internalization of BSEP is therefore sensitive to the treatment with chlorpromazine, an inhibitor of clathrin-mediated endocytosis (CME) [3]. On the other hand, the formation of MRP2-containing vesicles from the canalicular membrane is mediated by dynamin, an essential component of clathrin-dependent and independent endocytosis, but not by clathrin [3].

Under cholestatic conditions, the physiological recycling of these transporters is altered, leading to a decrease in their expression at the canalicular membrane and an increase in intracellular, vesicular compartments. This exacerbated endocytic internalization has been described in several experimental and clinical types of cholestasis, and was systematically associated with a failure in the secretion of the specific substrates of BSEP and MRP2; accordingly, this process is considered crucial for the pathogenesis of the cholestatic disease [4].

Estradiol 17 β-D-glucuronide (E17G) is an endogenous metabolite of estradiol whose plasma levels increase during pregnancy and was postulated as responsible for the pathogenesis of intrahepatic cholestasis of pregnancy as well as that associated to hormonal replacement therapy in susceptible women [5]. Administration of E17G to rats produces a dose-dependent, acute and reversible cholestasis, and it is considered an excellent, reproducible experimental model of cholestasis in general, and of pregnancy-induced cholestasis in particular [6].

Our group demonstrated that endocytosis of BSEP and MRP2 induced by E17G depends on the activation of critical signaling pathways, including “classical” (Ca^{+2}-dependent) protein kinase C (PKC) isoforms (cPKC) [7], phosphoinositide 3-kinase/protein kinase B (PI3K/Akt) [8], mitogen-activated protein kinases (MAPKs) of the $p38^{MAPK}$ and extracellular signal related kinase (ERK)1/2 types [9], estrogen receptor alpha (ER-α) [10], EGFR-Src [11], and GPR30-adenylyl cyclase-PKA [12]. The cPKC/ER-α/EGFR/$p38^{MAPK}$-signaling pathway plays a critical role in the

initial endocytic internalization of canalicular transporters that leads to cholestasis [7,9,10], whereas PI3K/Akt/ERK1/2 is responsible for maintaining canalicular transporters internalized [7–10].

In spite of the enormous progress made in the acknowledgment of the signaling pathways leading to the endocytosis and intracellular retention of canalicular transporters in cholestasis induced by E17G, the molecular mechanisms governing the endocytic process remain unknown, and their characterization represented the main aim of this work.

2. MATERIALS AND METHODS

2.1. Animals

Adult female Wistar rats were maintained on a standard laboratory diet and water *ad libitum* and housed in a temperature- and humidity-controlled environment under a constant 12-h light/dark cycle. All animals received humane care, according to the *Guide for the Care and Use of Laboratory Animals* (National Institutes of Health). Protocols were approved by the local animal welfare committee.

2.2 Experimental procedures and treatments

Isolated rat hepatocyte couplets (IRHC) were obtained as previously described [13]. To ascertain the role for clathrin on BSEP and MRP2 endocytosis, IRHC were pre-incubated with the inhibitor of CME, monodansylcadaverine (MDC, Sigma-Aldrich, 100 µM, 15 min) [14]. Additionally, CME was inhibited by a K^+ depletion protocol [15]. Briefly, IRHC were exposed to a hypotonic shock (L15/water, 1:1) for 5 min, and then incubated for 30 min in minimal media (20 mM Hepes at pH 7.5, 140 mM NaCl, 1 mM $CaCl_2$, 1 mM $MgSO_4$, 5.5 mM glucose and 0.5% BSA); control buffer was supplemented with 10 mM KCl. The caveolin dependence was ascertained by using filipin (Sigma-Aldrich, 10 µg/mL, 15 min), a cholesterol-binding agent that prevents caveolae vesicle formation and, at the concentration used here, inhibited endocytosis in the hepatocyte-derived human cell line HepG2 [16]; additionally, caveolin-dependent endocytosis was inhibited with genistein (Sigma-Aldrich, 200 µM, 15 min) [17]. After this pretreatments, IRHC were exposed to E17G (200 µM), or vehicle (dimethyl sulfoxide, DMSO) in controls, for 20 min.

Freshly isolated rat hepatocytes, obtained as previously described [18] were treated with small interfering RNA (siRNA) targeting AP2, and cultured in collagen sandwich configuration (SCRH) to allow a polarized conformation, as described [10]. After 72h, SCRH were treated with E17G (200 µM; 30 min), or vehicle in controls.

For synthesis of siRNA to inhibit AP2 function, four RNA duplexes (siRNA) targeting to mRNA of rat adaptor AP2 subunit µ1 (siRNA1, CATGCCTGCCATGCGCTTG), subunit µ2 (siRNA2, TTGACGCGAAAGGCATCCA), subunit α1 (siRNA3, CTGGCCAGTGTGCACATGCT) and subunit α2 (siRNA4, TTTCCCTTTAATTTGTAGG) were designed with WIsiRNA selection program [19]. The siRNA control was designed by scrambling the nucleotides of one of these specific targets. siRNAs were synthesized with Ambion's Silencer siRNA Kit (Ambion, Cambridge, MA).

In isolated and perfused livers (IPL), the perfusion protocol was as described [7]. Taurocholate (TC, 2.5 µM) and 1-chloro-2,4-dinitrobenzene (0.5 µM) were added to the perfusion medium for BS and dinitrophenylglutathione (DNP-SG) biliary secretion studies. After a 15-min equilibration period, MDC (100 µM), or its vehicle (DMSO) in controls, was added to the reservoir. Fifteen min later, a 5-min basal bile sample was collected, followed by an intraportal single injection (over a 1-min period) of E17G (2 µmol/liver, in 10% BSA in saline) or only the vehicle in controls, and bile was collected at 5-min intervals for an additional 20-min period.

In experiments involving whole animals, E17G (15 µmol/kg of b.w., in DMSO-10 % BSA in saline) was administered by femoral vein, and liver samples were taken after 20 min of E17G administration.

2.3. Assessment of BSEP and MRP2 secretory function

Functional changes in BSEP and MRP2 in IRHC under the treatments described above were evaluated by assessing the canalicular vacuolar accumulation (cVA) of cholyl-glycylamidofluorescein (CGamF), a fluorescent Bsep substrate, or glutathione methylfluorescein (GS-MF), a fluorescent Mrp2 substrate derived from 5- chloromethylfluorescein diacetate, as described [12]. Briefly, cells were exposed to 2 µM CGamF or 2.5 µM CMFDA for 15 min, and canalicular transport activity was assessed by quantifying the percentage of IRHC in the field displaying in their canalicular vacuoles enough fluorescent signal to make it visible under an inverted fluorescence microscope (Zeiss Axiovert 25), from a total of 250-300 couplets per preparation.

Functional status of MRP2 in SCRH was evaluated by assessing the initial transport rate (ITR) of GS-MF, as described [20]. This parameter is the slope of the initial linear phase of canalicular accumulation of this fluorescent substrate, assessed by quantitative time-lapse imaging, under an inverted fluorescence microscope [20].

In IPL, transport activities of BSEP and MRP2 were evaluated by measuring biliary TC and DNP-SG excretion, respectively. DNP-SG content was assessed in all samples by high-

performance liquid chromatography, using authentic standards. Total bile salt concentration was assessed using the 3α-hydroxysteroid dehydrogenase procedure, and the result was assumed as TC concentration.

2.4. Assessment of BSEP and MRP2 subcellular localization

To evaluate the intracellular distribution of BSEP and MRP2 after treatments, IRHC and SCRH were fixed, permeabilized, and incubated with antibodies against BSEP (Cat. # PC-064, Kamiya Biomedical Company, 1:100, 1 h) or MRP2 (M2III-6, Alexis Biochemicals, 1:100, 1 h), followed by incubation with the respective Cy2-conjugated secondary antibodies (Jackson ImmunoResearch, 1:200, 2 h). Canaliculi were delimited by staining pericanalicular F-actin with Alexa Fluor 568 phalloidin (Molecular Probes, 1:100, 2 h). For colocalization studies, IRHC and SCRH were incubated with the Ab to MRP2 and Abs to Rab5, AP2, clathrin or caveolin (Cell Signaling, 1:100, 1 h), followed by incubation with the secondary antibodies, as described above. Nuclei were stained with 1.5 μM 4,6-diamidino-2-phenylindole.

In whole animals and IPL experiments, a liver lobe was excised 20 min after E17G administration, frozen immediately in liquid nitrogen-precooled isopentane, and stored at -70°C, for further immunofluorescence and confocal microscopy analysis, as described previously [7].

Densitometric analysis of transporter distribution from confocal images was carried out along a line perpendicular to the canalicular vacuole (in IRHC samples), or to the canaliculi (in liver samples), using the ImageJ software, in an investigator-blinded fashion, as previously described [7].

For colocalization studies, confocal Z-stack images were obtained in control and E17G-treated IRHC and SCRH. The images were analyzed using the ImageJ software. AP2, Rab5, clathrin or caveolin positive structures in each single image were demarcated by setting a threshold in the corresponding channel to these proteins to define a mask. The fraction of MRP2 that localized at these structures was estimated by measuring the total intensity of fluorescence in the images generated by applying the logical function “AND” between the MRP2 image and the AP2, Rab5, clathrin or caveolin mask. The percentage of MRP2 that colocalized with each protein was calculated relating the total intensity of fluorescence at the AP2, Rab5, clathrin or caveolin positive structures for MRP2 to the corresponding total cell fluorescence. The inverse analysis, i.e., setting of the threshold on the images to define a mask for MRP2, followed by the above described procedure, was performed to estimate the percentage of total cell AP2, Rab5, clathrin or caveolin colocalizing with MRP2.

2.5. Preparation of detergent soluble and insoluble plasma membrane fractions

From liver homogenates, fractions enriched in plasma membranes were prepared by ultracentrifugation at 200,000g for 60 min on a discontinuous 1.3 mol/L sucrose gradient, as described [21,22]. Lack of contamination of these membrane fractions with microsomal membranes had been previously demonstrated by assessing the enzymatic activity of the hepatic subcellular markers, 5´-nucleotidase (plasma membrane), acid phosphatase (lysosomes), aspartate aminotransferase (mitochondria), and glucose-6-phosphatase (microsomes) [21,22]. To further confirm the purity of the plasma membranes obtained, we assessed by western blot the expression of the early and recycling endosomal markers, Rab5 and Rab11, respectively, and they were virtually absent of this fraction (data not shown).

Purified plasma membranes thus obtained were resuspended in buffer (20 mM Tris-HCl [pH 7.4], 150 mM NaCl, 1 mM ethylene diamine tetraacetic acid (EDTA), and a mixture of protease inhibitors), containing 1% (final concentration) Triton X-100 (Sigma-Aldrich), and incubated on ice for 30 min. Insoluble components were spun down at 18,000g for 60 min, and the supernatant (containing Triton X-100 soluble proteins) were collected in a new tube. The pellets were resuspended in solubilization buffer (50 mM Tris-HCl [pH 8.8], 5 mM EDTA, and 1% sodium dodecyl sulfate) and homogenized. After acetone precipitation, soluble (non-raft microdomains) and insoluble (raft microdomains) fractions were processed for western blotting [23].

2.6. Immunoblotting

Western blots of membrane fractions were performed by using the previously described antibodies to BSEP, MRP2, caveolin-1, mouse β-actin and clathrin, and the corresponding horseradish peroxidase-conjugated secondary antibodies (Thermo Scientific, Rockford, IL). Protein bands were detected by an enhanced chemiluminescence detection system (Thermo Scientific). Autoradiographs were obtained by exposing the membranes to Amersham Hyperfilm ECL (GE Healthcare Limited, Chalfont St. Giles, UK). Densitometric analysis of the developed bands was performed using ImageJ Software.

2.7. Statistical analysis

One-way ANOVA, followed by Newman-Keuls' test, was used for multiple comparisons. The variances of the densitometric profiles of BSEP and MRP2 localization were compared with the Mann–Whitney U test. Values of $p < 0.05$ were considered to be statistically significant.

3. RESULTS

3.1. Impairment of secretory function and localization of BSEP and MRP2 induced by E17G in IRHC is prevented by inhibitors of CME

Transport activity of BSEP and MRP2 in IRHC was evaluated by analyzing the cVA of their fluorescent substrates CGamF and GS-MF, respectively. The decrease in cVA of CGamF and GS-MF induced by E17G was prevented by the specific inhibition of CME in IRHC pre-treated either with MDC or with a K^+ depletion protocol. In contrast, in IRHC pre-treated with filipin or genistein, two specific inhibitors of caveolin-mediated endocytosis, a significant decrease in the cVA of both fluorophores was observed, similar to that induced by E17G (Figure 1).

Figure 2A shows representative confocal images showing that E17G induced a redistribution of the canalicular transporters MRP2 and BSEP (green) from the canalicular zone (delimited by the pericanalicular actin network, in red) into intracellular vesicles (white arrows). This phenomenon was totally prevented by the blockade of the CME with MDC. This was confirmed by densitometric analysis of the fluorescence associated with the transporters (Figure 2B). None of the treatments modified actin distribution (Figure 2B). MDC itself did not modify the normal distribution of the transporters (data not shown).

3.2. E17G increases the colocalization of MRP2 with proteins involved in CME

Representative confocal images of the colocalization of clathrin (A), AP2 (B), and Rab5 (C) with MRP2 in IRHC and SCRH are shown in Figures 3 and 4, respectively.

In the color panels of Figure 3, depicting the merge between MRP2 staining and clathrin, AP2, and Rab5 masks, respectively, it can be observed that, under E17G treatment, MRP2 increases its colocalization with these proteins, mainly in the zone where intracellular vesicles are localized (amplified insets). Quantitative analysis confirmed a significant increase in the percentage of colocalization between MRP2 and these proteins in the E17G group (bar plots on the right). The percentage of clathrin, AP2, and Rab5 colocalizing with MRP2 was also increased when we performed the reverse analysis, *i.e.*, colocalization of clathrin, AP2, and Rab5 with MRP2 mask (data not shown). Like happened in IRHC, in SCRH, the colocalization of these proteins with MRP2 was significantly higher under E17G treatment, as compared with the control (Figure 4A, B, and C). On the other hand, colocalization of caveolin with MRP2 showed an important decrease in E17G-treated IRHC (Figure 3D).

For colocalization studies, both antibodies to the transporters (BSEP and MRP2) and the proteins of interest must be developed in different hosts. Since no commercial mouse antibodies to rat clathrin, Rab5, and AP2 are available, we bought the only commercial mouse antibody with

reported reactivity to rat BSEP [BSEP (F-6) antibody, sc-74500, Santa Cruz Biotechnology], but we failed to obtain positive immunofluorescent staining of BSEP using this antibody.

3.3. AP2 knock-down inhibits the endocytosis of BSEP and MRP2 induced by E17G

AP2 plays a crucial role in the machinery of CME. In order to confirm our findings using inhibitors of this endocytic pathway, the effect of E17G on the localization of BSEP and MRP2 was evaluated in SCRH transfected with siRNA targeting to rat AP2 mRNA. Experiments of knock down of AP2 with siRNA were performed in SCRH since this primary culture remains viable for a time period that allows the siRNA to silence the gene of interest. Unlike the IRHC model, the SCRH model also gives a protein yield that allows protein expression detection by western blot. Four different siRNAs were tested and siRNA1, which induced the more significant decrease in AP2 protein expression, was chosen for function and localization studies (Figure 5A).

Supporting a crucial role for AP2 in E17G-induced endocytosis of canalicular transporters, confocal images of the transfected SCRH show that the alteration in the localization of MRP2 and BSEP induced by E17G (Figure 5B, white arrows) were prevented in those cells effectively transfected with the siRNA against the AP2 µ1-adapting subunit. Besides, the knock-down of AP2 prevented the functional alteration of MRP2 induced by E17G, as assessed by the ITR of GS-MF, reaching transport values not significantly different from control SCRH (Figure 5C). On the other hand, in SCRH treated with E17G, the ITR of GS-MF decreased approximately 50% as compared to controls.

3.4. MDC prevents biliary secretory alterations and the endocytosis of BSEP and MRP2 induced by E17G in IPL

Administration of E17G to IPL produces a decrease in BF to approximately 40% of basal values (Figure 6A). This decrease is accompanied by a significant diminution in the biliary excretion of the substrates of MRP2 (Figure 6B) and BSEP (Figure 6C), DNP-SG (40% of basal) and TC (70% of basal), respectively. The activity of both transporters begins to recover after 15 min of E17G administration. In IPL pre-treated with MDC, the alteration in BF and TC excretion induced by E17G was partially but significantly prevented, while the alteration produced in the excretion of DNP-SG was totally prevented (Figure 6).

In IPL treated with E17G, both transporters are detected in intracellular structures, compatible with endocytic vesicles (Figure 7A, white arrows). This internalization was prevented in those IPL that were perfused with MDC, which showed a similar pattern of distribution to control. The densitometric studies of the images show that, under treatment with E17G, the distribution curve

of the transporters becomes flatter and wider, due to the increase of transporter-associated green fluorescence in a farthest zone from the canalicular membrane (Figure 7B). In IPL perfused with MDC and treated with E17G, the distribution pattern of both transporters was similar to control. None of the treatments modified the canalicular structure, evaluated by occludin distribution. MDC *per se* did not induce changes in the distribution of the transporters (data not shown).

3.5. E17G alters the distribution of BSEP and MRP2 between rafts and non-raft microdomains

BSEP and MRP2 are mostly found in rafts under normal conditions [24]. In fact, there is a positive correlation between membrane cholesterol content and the activity of both BSEP and MRP2 [25]. CME occurs from non-raft microdomains, which possess the machinery necessary for this mechanism. Therefore, for E17G to induce CME of transporters, they should be enriched in non-raft microdomains. To verify this contention, raft (high cholesterol) and non-raft (low cholesterol) plasma membrane microdomains were isolated based on their differential detergent solubility, and their purity was assessed by performing western blot of the raft-marker protein caveolin-1 and the non-raft-marker protein clathrin, as described in Materials and Methods and shown in Figure 8A.

BSEP and MRP2 were found enriched in raft microdomains (60% BSEP, 75% MRP2), both under basal conditions and after 20 min of vehicle injection in controls. However, in those rats who were injected with E17G, a switch of these transporters occurred in the membrane microdomains, leading to their enrichment in non-raft microdomains; BSEP was expressed 22% in rafts and 78% in non-rafts, while MRP2 was expressed approximately 18% and 82% in rafts and non-rafts, respectively (Figure 8B and C).

4. DISCUSSION

Exacerbated endocytosis of canalicular transporters with intracellular retention in endosomal compartments has been reported in numerous experimental cholestatic conditions, and, more importantly, in several human cholestatic pathologies [4]. Although this mechanism has been recognized as a causal phenomenon leading to impaired canalicular secretion, the molecular mechanisms triggering it, as well as the endocytic machinery involved, are still unknown. In this work, we gathered evidence demonstrating that, in E17G-induced cholestasis, the canalicular transporters BSEP and MRP2 undergo exacerbated endocytic internalization by CME, and that this could be associated with a shift of transporters from caveolin-enriched plasma membrane microdomains (rafts) to clathrin-enriched ones (non-rafts).

Several lines of evidence in different models for the study of bile secretion have been provided

here for the selective involvement of clathrin, but not caveolin, in E17G-induced BSEP/MRP2 endocytosis, namely *1*) Inhibition of caveolin-dependent endocytosis with filipin was without effect; filipin sequesters cholesterol from lipid rafts, and cholesterol is required for caveolae to form [26]; *2*) different maneuvers leading to CME blockage by unrelated mechanisms, such as administration of MDC or K^+ depletion in IRHC (or the first in IPL); MDC is a potent inhibitor of transglutaminase, a cross-linking enzyme necessary for clustering of the endocytosed protein in the region of clathrin-coated membrane regions and in the coated pits [27], whereas K^+ depletion induces drastic changes in the distribution of clathrin by removing plasma membrane-associated clathrin lattices into "microcages" beneath the plasma membrane [28]; *3*) Inhibition of E17G-induced canalicular transporter internalization was also apparent when CME was blocked by knocking down μ1-subunit of AP2 with siRNA; AP2 is an adaptor complex that triggers formation of the clathrin lattice, and mediates interaction between clathrin and the cargo protein [29]; *4*) After being endocytosed, MRP2 colocalized with clathrin, AP2, as well as with Rab5; this small GTPase regulates not only the dynamic of early endosome where cargo is sorted after CME but also fusion of clathrin-coated vesicles with these early endosomes [30].

The clathrin dependence of BSEP and MRP2 endocytosis in E17G-induced cholestasis is somewhat unexpected due to the preferential normal localization of these transporters in raft microdomains, which are enriched in caveolin rather than clathrin [24,25]. However, the preferential association of a plasma membrane protein with rafts is not a determinant of their endocytosis via the caveolin-dependent mechanism [31]. Actually, BSEP is constitutively internalized via CME, with its C-terminal tyrosine motif (conserved in all the members of the ABC superfamily) being key for interaction with AP2 [2]. Furthermore, silencing AP2 expression in 3xFlag-BSEP-expresing HeLa cells and in human SCRH inhibited internalization of BSEP [32], and *in vivo* studies demonstrated that constitutive BSEP internalization was inhibited after pharmacological impairing of the expression of AP2 α- and μ2-adaptin subunits with 4-phenylbutyrate in rat and human liver [33].

The mechanisms underlying constitutive MRP2 internalization are far less studied, but the studies carried out suggested a differential behavior with BSEP. In the T-Rex 293 cell line from embryonic human kidney with both BSEP and MRP2 expressed *ad hoc*, BSEP, but no MRP2 endocytosis, was sensitive to the inhibitor of CME chlorpromazine [3]. MRP2 was instead sensitive to dynasore, a dynamin inhibitor; dynamin play a role both in coated pit scission and in linking internalization and actin cytoskeleton in both clathrin-dependent and independent endocytosis [34]. If these results would be valid for hepatocytes, and extrapolated to rat MRP2, they would suggest that constitutive endocytosis of MRP2 would be different from the endocytosis

under cholestasis conditions.

CME requires the interaction of the protein to be endocytosed with AP2, an interaction that is usually done through tyrosine or leucine motifs present at the N or C-terminal domains of the endocytosed protein [35], as described for the constitutive endocytosis of BSEP. Lack of clathrin dependence of constitutive MRP2 endocytosis suggests that AP2-interaction domains could not be present in its structure, thus not allowing its recruitment under physiological conditions. However, it is possible that, in a cholestatic context, activation of signaling pathways that have MRP2 as a target could induce postransductional modifications on the transporter, which can make possible the establishment of unconventional interactions with clathrin. Supporting this possibility, it has been recently reported that CME of the K^+ Kv1.3 channel in HeLa cells depends on its C-terminal domain phosphorylation mediated by ERK1/2, after activation of this kinase by EGF [36]. Alternatively, it could be possible that E17G induces the endocytosis of MRP2 by a non-conventional mechanism different from the interaction of AP2 with tyrosine or di-leucine domains, interacting through different domains enabled by the phosphorylation of MRP2 through one of the pro-cholestatic signaling pathways involved in E17G-induced cholestasis. In line with this, a phosphorylation site for PKC, at the C-terminal of MRP2 (Ser^{1542}), has been reported [37]. Interestingly, different PKC isoforms have been shown by our group and others to be involved in the endocytic internalization of MRP2 in different models of cholestasis, including those induced by E17G [7], oxidative stress [38], and taurolithocholate [39].

In addition, our group has also provided evidence for the participation of $p38^{MAPK}$ in the endocytosis of canalicular transporters in E17G-induced cholestasis [9]. This kinase has been reported to accelerate CME of several membrane receptors, such as EGFR [40]. Like this, BSEP is internalized by CME through a mechanism involving AP2, a protein whose phosphorylation by $p38^{MAPK}$ is essential for the recruitment of the cargo towards the clathrin-coated depressions during endocytosis of EGFR [41]. Furthermore, another possible target of $p38^{MAPK}$ is Rab-GDP (Rab-GDI dissociation inhibitor), a protein that stimulates the recycling of Rab5 between the membrane and the cytosol, thereby increasing the endocytic rate [42].

Exacerbated CME in cholestasis of transporters that, like BSEP and MRP2, mostly reside in rafts microdomains, may involve migration of these transporters to non-rafts microdomains, where they can undergo CME. Our results suggest that this could be the case. In line with our finding, Marrone *et al.* have recently reported a similar redistribution of BSEP from raft to non-raft microdomains in 17α-ethynylestradiol (EE)-induced cholestasis in rats, and this was suggested to contribute to the alteration of BSEP activity in this pathology [23]. Interestingly, our group reported that glucuronidation of EE is an essential requirement for it to exert its cholestatic effect

[43]. Thus, it is possible to postulate that, in EE cholestasis, its D-ring glucuronide, which is a potent acute cholestatic with similar cholestatic mechanisms to E17G [44], is responsible for the redistribution of BSEP from raft to non-raft microdomains, and the associated secretory failure induced by EE. Suggestively, in EE-induced cholestasis, MRP2 and BSEP decrease their protein expression without changes in their mRNA [45,46]. Accordingly, this postrancriptional downregulation could be a consequence of the continuous formation of the glucuronide metabolite of EE during the 5-day treatment, which would induce a sustained endocytosis of MRP2 and BSEP, leading to lysosomal degradation.

It remains to ascertain the molecular mechanisms by which these metabolites could have induced a shift of canalicular transporters between different membrane microdomains. There are different ways by which a protein is preferentially integrated into raft microdomains: *i)* by lipidation (protein acylation, glycosylphosphatidylinositol binding or covalent attachment to cholesterol), *ii)* through protein-protein interactions with other proteins anchored to rafts, and *iii)* by having a consensus sequence of amino acid that recognizes and interacts with cholesterol, referred to as "CRAC" domain (cholesterol recognition/interaction amino acid consensus). All these processes can be, hypothetically, modulated by acute metabolic changes mediated by signaling pathways, leading to modifications of the protein-protein interactions or affinity of CRAC domains for cholesterol [47]. In transmembrane proteins like transporters, the existence of a CRAC domain is the most likely cause of preferential localization in lipid rafts [47]. Although the existence of CRAC domains in BSEP and MRP2 has not yet been investigated, five of these domains exist in another ABC transporter, BCRP (ABCG2), and they explain the dependence of their activity on membrane cholesterol [47]. Bearing in mind that transport activity of both BSEP [25] and MRP2 [48] critically depends on the membrane cholesterol content, the existence of domains for interaction with cholesterol in their structure is indeed likely.

Another possible target of E17G that could facilitate the shift of BSEP and MRP2 from raft to non-raft microdomains is radixin, a protein of the ERM family that anchors BSEP and MRP2 to the canalicular membrane, linking them to the actin cytoskeleton. Disorganization of radixin occurs in EE cholestasis and, since EE glucuronide is the causative agent in this pathology, it is possible that the same holds true for E17G cholestasis. In general terms, maintenance of lipid and protein compartmentalization in raft and non-raft microdomains depends crucially on the integrity of the actin cytoskeleton, whose depolymerization leads to homogenization of the plasma membrane [49]. Disruption of the hepatocellular distribution of ezrin (a member of the ERM family) by keratin 8 knockdown was associated with profound changes in the organization of membrane rafts, and in a redistribution of FasR, a protein located in raft microdomains [50]. The

raft microdomains themselves (including their lipid components) become more mobile when the binding of some of their constituent proteins to the actin cytoskeleton is lost, as has been shown for Cbp/PAR protein [51].

Migration from raft to non-raft microdomains can also affect the intrinsic activity of transporters that may be temporarily retained in this microenvironment. For instance, BSEP activity is positively related to the cholesterol content in the membrane, and therefore BSEP activity is much higher in rafts, where the carrier is enriched under physiological conditions [25]. Therefore, BSEP shift from rafts to non-raft lipid microdomains, as shown here for E17G and previously for EE by Marrone *et al* [23], may represent itself a novel cholestatic mechanism that impairs BSEP intrinsic activity, complementary to the exacerbation of BSEP endocytosis induced by the same shift, which reduces the density of the carrier in the canalicular membrane. Interestingly, bile salt excretion via BSEP was restored by anchoring the transporter to raft microdomains via hepatic gene transfer of human aquaporin-1 to these microdomains in the canalicular membrane of EE cholestatic rats [23], thus highlighting the crucial impact that migration from rafts to non-rafts microdomains have for BSEP function in cholestasis. In contrast, MRP2 activity appears to be less influenced by the lipid microenvironment, as suggested by studies in HepG2 showing that its transport function depends on membrane cholesterol content but not on its presence in detergent-resistant microdomains [48]. This differential effect could explain why the inhibition of CME in IPL did not completely prevent the decrease in bile salt excretion induced by E17G, as did it for the MRP2 substrate DNP-SG (see Fig 5B). Another possible factor that could explain the selective inhibition of BSEP by E17G in MDC-treated IPL is the well-recognized transinhibition of BSEP by E17G, once excreted into the canaliculus via MRP2 [52]; in our model, where the inhibition of the transport function of MRP2 by E17G is completely prevented by MDC, such a transinhibition would be fully operative.

5. CONCLUSION

Our findings clearly demonstrate that CME is the mechanism responsible for the internalization of the canalicular transporters BSEP and MRP2 in E17G-induced cholestasis (Figure 9). In addition, we provided the first line of evidence of changes in the distribution of these transporters in membrane microdomains that could justify, at least partially, the increase of their endocytosis in this and possibly in other models of cholestasis. Clearly, further studies are needed to confirm and clarify the mechanisms that affect the localization of these transporters in their membrane microdomains, as well as the signaling pathways that trigger this process. Irrespective of these limitations, the generalized occurrence of canalicular transporter internalization as a

physiopathological mechanism in most types of experimental and clinical cholestasis points clathrin and other components of CME machinery as new potential targets for future pharmacological strategies in cholestasis therapeutics.

Funding: This work was supported by grants from Agencia Nacional de Promoción Científica y Tecnológica (PICT 2013 N° 0974) and Consejo Nacional de Investigaciones Científicas y Técnicas (PIP 2013 N° 0217), ARGENTINA.

REFERENCES

[1] Y. Wakabayashi, Transporters on Demand: Intracellular Reservoirs and Cycling of Bile Canalicular ABC Transporters, J. Biol. Chem. 281 (2006) 27669–27673. doi:10.1074/jbc.R600013200.

[2] P. Lam, S. Xu, C.J. Soroka, J.L. Boyer, A C-terminal tyrosine-based motif in the bile salt export pump directs clathrin-dependent endocytosis., Hepatology. 55 (2012) 1901–11. doi:10.1002/hep.25523.

[3] K. Aida, H. Hayashi, K. Inamura, T. Mizuno, Y. Sugiyama, Differential roles of ubiquitination in the degradation mechanism of cell surface-resident bile salt export pump and multidrug resistance-associated protein 2, Mol Pharmacol. 85 (2014) 482–491. doi:10.1124/mol.113.091090 mol.113.091090 [pii].

[4] F.A. Crocenzi, A.E. Zucchetti, A.C. Boaglio, I.R. Barosso, E.J. Sanchez Pozzi, A.D. Mottino, M.G. Roma, Localization status of hepatocellular transporters in cholestasis, Front Biosci. 17 (2012) 1201–1218. doi:3981 [pii].

[5] M. Vore, Y. Liu, L. Huang, Cholestatic properties and hepatic transport of steroid glucuronides, Drug.Metabol.Rev. 29 (1997) 183–203.

[6] M. Meyers, W. Slikker, G. Pascoe, M. Vore, Characterization of cholestasis induced by estradiol-17 beta-D-glucuronide in the rat, J. Pharmacol. Exp. Ther. 214 (1980) 87–93.

[7] F.A. Crocenzi, E.J. Sanchez Pozzi, M.L. Ruiz, A.E. Zucchetti, M.G. Roma, A.D. Mottino, M. Vore, Ca(2+)-dependent protein kinase C isoforms are critical to estradiol 17beta-D-glucuronide-induced cholestasis in the rat, Hepatology. 48 (2008) 1885–1895.

[8] A.C. Boaglio, A.E. Zucchetti, E.J. Sanchez Pozzi, J.M. Pellegrino, J.E. Ochoa, A.D. Mottino, M. Vore, F.A. Crocenzi, M.G. Roma, Phosphoinositide 3-kinase/protein kinase B signaling pathway is involved in estradiol 17beta-D-glucuronide-induced cholestasis: complementarity with classical protein kinase C, Hepatology. 52 (2010) 1465–1476.

[9] A.C. Boaglio, A.E. Zucchetti, F.D. Toledo, I.R. Barosso, E.J. Sánchez Pozzi, F.A. Crocenzi, M.G. Roma, ERK1/2 and p38 MAPKs are complementarily involved in estradiol 17ß-D-glucuronide-induced cholestasis: crosstalk with cPKC and PI3K., PLoS One. 7 (2012) e49255. doi:10.1371/journal.pone.0049255.

[10] I.R. Barosso, A.E. Zucchetti, A.C. Boaglio, M.C. Larocca, D.R. Taborda, M.G. Luquita, M.G. Roma, F.A. Crocenzi, E.J. Sánchez Pozzi, Sequential Activation of Classic PKC and Estrogen Receptor α Is Involved in Estradiol 17ß-D-Glucuronide-Induced Cholestasis, PLoS One. 7 (2012).

[11] I.R. Barosso, A.E. Zucchetti, G.S. Miszczuk, A.C. Boaglio, D.R. Taborda, M.G. Roma, F.A. Crocenzi, E.J. Sánchez Pozzi, EGFR participates downstream of ERα in estradiol-17β-d-glucuronide-induced impairment of Abcc2 function in isolated rat hepatocyte couplets, Arch. Toxicol. 90 (2016) 891–903. doi:10.1007/s00204-015-1507-8.

[12] A.E. Zucchetti, I.R. Barosso, A.C. Boaglio, C.L. Basiglio, G. Miszczuk, M.C. Larocca, M.L. Ruiz, C.A. Davio, M.G. Roma, F.A. Crocenzi, E.J.S. Pozzi, G-protein-coupled receptor 30/adenylyl cyclase/protein kinase A pathway is involved in estradiol 17ß-D-glucuronide-induced cholestasis., Hepatology. 59 (2014) 1016–29. doi:10.1002/hep.26752.

[13] J.C. Wilton, D.E. Williams, A.J. Strain, R.A. Parslow, J.K. Chipman, R. Coleman, Purification of hepatocyte couplets by centrifugal elutriation, Hepatology. 14 (1991) 180–183. http://www.ncbi.nlm.nih.gov/pubmed/1906045 (accessed August 11, 2016).

[14] M. Krishnan, T.R. Kannan, J.B. Baseman, Mycoplasma pneumoniae CARDS toxin is internalized via clathrin-mediated endocytosis., PLoS One. 8 (2013) e62706. doi:10.1371/journal.pone.0062706.

[15] C. Meyer, P. Godoy, A. Bachmann, Y. Liu, D. Barzan, I. Ilkavets, P. Maier, C. Herskind, J.G. Hengstler, S. Dooley, Distinct role of endocytosis for Smad and non-Smad TGF-beta signaling regulation in hepatocytes, J Hepatol. 55 (2011) 369–378. doi:10.1016/j.jhep.2010.11.027S0168-8278(10)01178-5 [pii].

[16] A.-S. Zhang, F. Yang, K. Meyer, C. Hernandez, T. Chapman-Arvedson, P.J. Bjorkman, C.A. Enns, Neogenin-mediated hemojuvelin shedding occurs after hemojuvelin traffics to the plasma membrane., J. Biol. Chem. 283 (2008) 17494–502. doi:10.1074/jbc.M710527200.

[17] J. Rejman, A. Bragonzi, M. Conese, Role of clathrin- and caveolae-mediated endocytosis in gene transfer mediated by lipo- and polyplexes, Mol. Ther. 12 (2005) 468–474. doi:10.1016/j.ymthe.2005.03.038.

[18] M.N. Berry, D.S. Friend, High-yield preparation of isolated rat liver parenchymal cells: a biochemical and fine structural study, J Cell Biol. 43 (1969) 506–520.

[19] B. Yuan, R. Latek, M. Hossbach, T. Tuschl, F. Lewitter, siRNA Selection Server: an automated siRNA oligonucleotide prediction server., Nucleic Acids Res. 32 (2004) W130-4. doi:10.1093/nar/gkh366.

[20] G.S. Miszczuk, I.R. Barosso, A.E. Zucchetti, A.C. Boaglio, J.M. Pellegrino, E.J. Sánchez Pozzi, M.G. Roma, F.A. Crocenzi, Sandwich-cultured rat hepatocytes as an in vitro model to study canalicular transport alterations in cholestasis, Arch. Toxicol. 89 (2015) 979–990. doi:10.1007/s00204-014-1283-x.

[21] F.I. Carreras, S.A. Gradilone, A. Mazzone, F. Garcia, B.Q. Huang, J.E. Ochoa, P.S. Tietz, N.F. LaRusso, G. Calamita, R.A. Marinelli, Rat hepatocyte aquaporin-8 water channels are down-regulated in extrahepatic cholestasis, Hepatology. 37 (2003) 1026–1033.

[22] F. Garcia, A. Kierbel, M.C. Larocca, S.A. Gradilone, P. Splinter, N.F. LaRusso, R.A. Marinelli, The water channel aquaporin-8 is mainly intracellular in rat hepatocytes, and its plasma membrane insertion is stimulated by cyclic AMP, J. Biol. Chem. 276 (2001) 12147–12152.

[23] J. Marrone, L.R. Soria, M. Danielli, G.L. Lehmann, M. Cecilia Larocca, R.A. Marinelli, Hepatic Gene Transfer of Human Aquaporin-1 Improves Bile Salt Secretory Failure in Rats with Estrogen-Induced Cholestasis., Hepatology. (2016). doi:10.1002/hep.28564.

[24] M.G. Ismair, S. Hausler, C.A. Stuermer, C. Guyot, P.J. Meier, J. Roth, B. Stieger, ABC-transporters are localized in caveolin-1-positive and reggie-1-negative and reggie-2-negative microdomains of the canalicular membrane in rat hepatocytes, Hepatology. 49 (2009) 1673–1682.

[25] C.C. Paulusma, D.R. de Waart, C. Kunne, K.S. Mok, R.P.J.O. Elferink, Activity of the bile salt export pump (ABCB11) is critically dependent on canalicular membrane cholesterol content., J. Biol. Chem. 284 (2009) 9947–54. doi:10.1074/jbc.M808667200.

[26] K.G. Rothberg, J.E. Heuser, W.C. Donzell, Y.-S. Ying, J.R. Glenney, R.G.W. Anderson, Caveolin, a protein component of caveolae membrane coats, Cell. 68 (1992) 673–682. doi:10.1016/0092-8674(92)90143-Z.

[27] Y. Phonphok, K.S. Rosenthal, Stabilization of clathrin coated vesicles by amantadine, tromantadine and other hydrophobic amines., FEBS Lett. 281 (1991) 188–90.

http://www.ncbi.nlm.nih.gov/pubmed/1901801 (accessed July 26, 2017).

[28] J.E. Heuser, R.G. Anderson, Hypertonic media inhibit receptor-mediated endocytosis by blocking clathrin-coated pit formation., J. Cell Biol. 108 (1989) 389–400. http://www.ncbi.nlm.nih.gov/pubmed/2563728 (accessed July 26, 2017).

[29] H. Ohno, J. Stewart, M.C. Fournier, H. Bosshart, I. Rhee, S. Miyatake, T. Saito, A. Gallusser, T. Kirchhausen, J.S. Bonifacino, Interaction of tyrosine-based sorting signals with clathrin-associated proteins., Science. 269 (1995) 1872–5. http://www.ncbi.nlm.nih.gov/pubmed/7569928 (accessed July 26, 2017).

[30] E. Galperin, A. Sorkin, Visualization of Rab5 activity in living cells by FRET microscopy and influence of plasma-membrane-targeted Rab5 on clathrin-dependent endocytosis., J. Cell Sci. 116 (2003) 4799–810. doi:10.1242/jcs.00801.

[31] I.R. Nabi, P.U. Le, Caveolae/raft-dependent endocytosis, J. Cell Biol. 161 (2003) 673–677. doi:10.1083/jcb.200302028.

[32] H. Hayashi, K. Inamura, K. Aida, S. Naoi, R. Horikawa, H. Nagasaka, T. Takatani, T. Fukushima, A. Hattori, T. Yabuki, I. Horii, Y. Sugiyama, AP2 adaptor complex mediates bile salt export pump internalization and modulates its hepatocanalicular expression and transport function, Hepatology. 55 (2012) 1889–1900. doi:10.1002/hep.25591.

[33] H. Hayashi, Y. Sugiyama, 4-phenylbutyrate enhances the cell surface expression and the transport capacity of wild-type and mutated bile salt export pumps, Hepatology. 45 (2007) 1506–1516. doi:10.1002/hep.21630.

[34] N. Sauvonnet, A. Dujeancourt, A. Dautry-Varsat, Cortactin and dynamin are required for the clathrin-independent endocytosis of gammac cytokine receptor., J. Cell Biol. 168 (2005) 155–63. doi:10.1083/jcb.200406174.

[35] A. Sorkin, Cargo recognition during clathrin-mediated endocytosis: a team effort, Curr. Opin. Cell Biol. 16 (2004) 392–399. doi:10.1016/j.ceb.2004.06.001.

[36] R. Martínez-Mármol, N. Comes, K. Styrczewska, M. Pérez-Verdaguer, R. Vicente, L. Pujadas, E. Soriano, A. Sorkin, A. Felipe, Unconventional EGF-induced ERK1/2-mediated Kv1.3 endocytosis., Cell. Mol. Life Sci. 73 (2016) 1515–28. doi:10.1007/s00018-015-2082-0.

[37] T. Hegedüs, T. Sessler, R. Scott, W. Thelin, É. Bakos, A. Váradi, K. Szabó, L. Homolya, S.L. Milgram, B. Sarkadi, T. Hegedus, T. Sessler, R. Scott, W. Thelin, E. Bakos, A. Varadi, K. Szabo, L. Homolya, S.L. Milgram, B. Sarkadi, C-terminal phosphorylation of MRP2 modulates its interaction with PDZ proteins, Biochem Biophys Res Commun. 302 (2003) 454–461. doi:S0006291X03001967 [pii].

[38] S. Sekine, K. Ito, T. Horie, Oxidative stress and Mrp2 internalization, Free Radic. Biol. Med. 40 (2006) 2166–2174. doi:10.1016/j.freeradbiomed.2006.02.015.

[39] U. Beuers, I. Probst, C. Soroka, J.L. Boyer, G.A. Kullak-Ublick, G. Paumgartner, Modulation of protein kinase C by taurolithocholic acid in isolated rat hepatocytes, Hepatology. 29 (1999) 477–482.

[40] S. Vergarajauregui, A. San Miguel, R. Puertollano, Activation of p38 mitogen-activated protein kinase promotes epidermal growth factor receptor internalization, Traffic. 7 (2006) 686–698. doi:TRA420 [pii]10.1111/j.1600-0854.2006.00420.x.

[41] M. V. Grandal, L.M. Grøvdal, L. Henriksen, M.H. Andersen, M.R. Holst, I.H. Madshus, B. van Deurs, L.M. Grovdal, L. Henriksen, M.H. Andersen, M.R. Holst, I.H. Madshus, B. van

Deurs, Differential Roles of Grb2 and AP-2 in p38 MAPK- and EGF-Induced EGFR Internalization, Traffic. 13 (2011) 576–585. doi:10.1111/j.1600-0854.2011.01322.x.

[42] J.L. Seachrist, S.S. Ferguson, Regulation of G protein-coupled receptor endocytosis and trafficking by Rab GTPases, Life Sci. 74 (2003) 225–235. doi:S0024320503008282 [pii].

[43] F.A. Crocenzi, J.M. Pellegrino, V.A. Catania, M.G. Luquita, M.G. Roma, A.D. Mottino, E.J. Sanchez Pozzi, Galactosamine prevents ethinylestradiol-induced cholestasis, Drug Metab Dispos. 34 (2006) 993–997.

[44] M. Vore, H. Hadd, W. Slikker Jr., Ethynylestradiol-17 á D-ring glucuronide conjugates are potent cholestatic agents in the rat, Life Sci. 32 (1983) 2989–2993.

[45] M. Trauner, M. Arrese, C.J. Soroka, M. Ananthanarayanan, T.A. Koeppel, S.F. Schlosser, F.J. Suchy, D. Keppler, J.L. Boyer, The rat canalicular conjugate export pump (Mrp2) is down-regulated in intrahepatic and obstructive cholestasis, Gastroenterology. 113 (1997) 255–264.

[46] J.M. Lee, M. Trauner, C.J. Soroka, B. Stieger, P.J. Meier, J.L. Boyer, Expression of the bile salt export pump is maintained after chronic cholestasis in the rat, Gastroenterology. 118 (2000) 163–172.

[47] Z. Gál, C. Hegedüs, G. Szakács, A. Váradi, B. Sarkadi, C. Özvegy-Laczka, Mutations of the central tyrosines of putative cholesterol recognition amino acid consensus (CRAC) sequences modify folding, activity, and sterol-sensing of the human ABCG2 multidrug transporter, Biochim. Biophys. Acta - Biomembr. 1848 (2015) 477–487. doi:10.1016/j.bbamem.2014.11.006.

[48] K. Ito, D. Hoekstra, S.C.D. van Ijzendoorn, Cholesterol but not association with detergent resistant membranes is necessary for the transport function of MRP2/ABCC2., FEBS Lett. 582 (2008) 4153–7. doi:10.1016/j.febslet.2008.11.013.

[49] A. Honigmann, A. Pralle, Compartmentalization of the Cell Membrane., J. Mol. Biol. 428 (2016) 4739–4748. doi:10.1016/j.jmb.2016.09.022.

[50] S. Gilbert, A. Loranger, J.N. Lavoie, N. Marceau, Cytoskeleton keratin regulation of FasR signaling through modulation of actin/ezrin interplay at lipid rafts in hepatocytes, Apoptosis. 17 (2012) 880–894. doi:10.1007/s10495-012-0733-2.

[51] K. Itoh, M. Sakakibara, S. Yamasaki, A. Takeuchi, H. Arase, M. Miyazaki, N. Nakajima, M. Okada, T. Saito, Cutting edge: negative regulation of immune synapse formation by anchoring lipid raft to cytoskeleton through Cbp-EBP50-ERM assembly., J. Immunol. 168 (2002) 541–4. http://www.ncbi.nlm.nih.gov/pubmed/11777944 (accessed November 7, 2016).

[52] B. Stieger, K. Fattinger, J. Madon, G.A. Kullak-Ublick, P.J. Meier, Drug- and estrogen-induced cholestasis through inhibition of the hepatocellular bile salt export pump (Bsep) of rat liver, Gastroenterology. 118 (2000) 422–430.

FIGURE LEGENDS

Figure 1: Effect of clathrin- or caveolin-dependent endocytosis inhibitors on the canalicular vacuolar accumulation (cVA) of GS-MF (MRP2 substrate, panel A) and CGamF (BSEP substrate, panel B). IRHC were pre-incubated for 15 min with vehicle (in control) or maneuvers leading to inhibition of different endocytic pathways, *i.e.*, MDC exposure (100 µM, 15 min) and K^+ depletion protocol for the clathrin-mediated pathway, and filipin exposure (10 µg/µL, 15 min) or genistein incubation (200 µM, 15 min) for the caveolin-mediated ones. Then, IRHC were exposed to E17G for a further 20-min period. cVA was calculated from microphotographs, as the percentage of IRHC with visible fluorescence in their canalicular vacuoles, with respect to the total IRHC present in each field, and referred to control values. Under control conditions, 65-70% of the IRHC analyzed were positive for vacuolar fluorescent signal, depending on the preparation. Data are expressed as mean ± S.D. (n = 250/300 IRHC per preparation, from at least 3 independent experiments). *Significantly different from control (p <0.05). $^{\#}$Significantly different from genistein group.

Figure 2: MDC prevents the endocytosis of the canalicular transporters MRP2 and BSEP induced by E17G in IRHC. A. Representative confocal images of IRHC showing the distribution of transporters (green) and the pericanalicular actin network (red)**.** In control conditions, the fluorescence associated with the transporters is mostly localized in the canalicular zone. E17G (200 µM) induces internalization of these transporters, visualized in vesicles beyond the actin limits (white arrows). A similar pattern of transporter internalization was observed in IRHC pre-treated with filipin (25 µg/mL), and then incubated with E17G. The effect of E17G was significantly prevented by pre-treatment with MDC (100 µM). **B.** Densitometric analysis of images was performed along a line perpendicular to the canalicular vacuole (4 µM to each side of the vacuole center), by using ImageJ software. A schematic representation of this procedure is shown (inset), where the center of the canalicular vacuole is represented by a dotted line. The limits of the canalicular space were identified by F-actin-associated fluorescence (B, right). Each profile was normalized to the sum of all intensities of the respective measurement. Under E17G treatment, these profiles were wider and flatter, compatible with an increment in transporter-associated fluorescence beyond the limits of the canalicular vacuole. Statistical analysis of the differences in the distribution patterns revealed a significant internalization of transporters under E17G treatment ($p < 0.05$ *vs.* control), which was completely abolished by MDC ($p < 0.05$ *vs.* E17G). None of the treatments affected the normal distribution of actin. Results are expressed as

mean ± S.E.M. *n* = 6–8 randomly selected canalicular vacuoles per preparation, from 3 independent preparations.

Figure 3: **Colocalization of MRP2 with proteins involved in clathrin-dependent endocytic machinery in IRHC.** Double immunofluorescent labeling of MRP2 (green) and clathrin (**A**, red), AP2 (**B**, red), Rab 5 (**C**, red) or caveolin (**D**, red) was performed in IRHC. Confocal z-stacks of control IRHC and those treated with E17G (200 µM, 20 min) were taken. E17G treatment did not affect clathrin, AP2, Rab5 and caveolin cellular distribution. Amplified images of the pericanalicular region with clathrin (A), AP2 (B), Rab5 (C), caveolin (D), and MRP2 in monochrome, and the merge between MRP2 and each of these proteins in color, are shown; in these insets, it can be observed an increment in the colocalization of MRP2 with clathrin, AP2, and Rab5 (visualized as yellow staining), as well as a decrease in colocalization between MRP2 and caveolin (D), in E17G-treated IRHC. Colocalization analysis of the stacks was performed with the Image J software. AP2, Rab5, clathrin, or caveolin positive structures were demarcated by setting a threshold to define a mask. The fraction of MRP2 that localized at these structures was estimated by measuring the total intensity of fluorescence in the images generated by applying the logical function "AND" between the MRP2 image and the AP2, Rab5, clathrin, or caveolin mask. In E17G-treated IHRC, a higher percentage of colocalization of MRP2 with the proteins involved in CME (bar plots in A, B, and C) and a decrease in the colocalization of MRP2 with caveolin (bar plot in D) was observed. Results are expressed as mean ± S.D. **p* <0.05 *vs* control, *n* = 10 from 3-5 different independent preparations. Scale bar = 3 µm.

Figure 4: Colocalization of MRP2 with proteins involved in clathrin-dependent endocytic machinery in SCRH. Double immunofluorescent labeling of MRP2 (green) and clathrin (A, red), AP2 (B, red), or Rab 5 (C, red) was performed in SCRH. Confocal z-stacks of control SCRH and those treated with E17G (200 µM, 20 min) were taken. E17G treatment did not affect clathrin, AP2, and Rab5 cellular distribution, while endocytosis of MRP2 can be clearly visualized. In representative images of the overlapping between the MRP2 and the proteins of interest, it can be observed an increase in the colocalization of MRP2 with all these proteins in the pericanalicular zone under E17G treatment (insets). Colocalization analysis of the stacks was performed with the Image J software. In SCRH treated with E17G, a higher percentage of colocalization MRP2 with the proteins involved in CME was observed (bar plots). Results are expressed as mean ± S.D. **p* <0.05 *vs.* control, *n* = 10 from 3-5 different independent preparations. Scale bar = 10 µm.

Figure 5: Knock down of AP2 in SCRH prevents impairment of localization and transport activity of MRP2 induced by E17G. SCRH were transfected with AP2 siRNA and RNA SC for 48 h. **A.** Representative western blot of AP2 in transfected SCRH. siRNA 1, 2, and 3 induced a significant decrease of AP2 expression. Results are expressed as mean ± S.D. * $p < 0.05$ *vs.* SC, $n = 3$. **B.** Representative confocal images showing the distribution of MRP2 (green) in SCRH under different treatments. The canalicular zone is delimited by occludin (red) and the nuclei are shown in blue. In scrambled control (SC)-treated SCRH, the fluorescence associated with the transporter is confined to the canalicular space. E17G induced a clear internalization of vesicles containing the transporter beyond the canalicular limits in these cells (white arrows). In cells transfected with siRNA1 and treated with E17G, the internalization was clearly prevented. The siRNA *per se* had no effect on the distribution of MRP2 (data not shown). **C.** Initial transport rate (ITR) of the MRP2 substrate GS-MF. After transfection for 48hs, SCRH were exposed for 30 min to E17G (200 µM), or its vehicle in controls, and then to 5-chloromethylfluorescein diacetate, a GS-MF precursor. The slope of the curve obtained by plotting the fluorescence intensity associated with GS-MF of 70-100 pseudo-canaliculi *vs.* time from 3 different preparations was used to estimate ITR of GS-MF, which was corrected by canalicular width. Data were expressed as mean ± S.D. *$p < 0.05$ *vs.* SC.

Figure 6: MDC prevents alteration of biliary flow and biliary excretion of MRP2 and BSEP substrates induced by E17G in IPL. The graphs show the temporal changes in biliary flow (A), and biliary excretion of DNP-SG (B) and TC (C), during the perfusion period. IPL were treated with a single bolus dose of E17G (2 µmol/liver), or its vehicle in controls, in the presence or absence of MDC (200 µM) in the perfusion medium. E17G was administered after 15 min of perfusion with MDC or its vehicle, and bile was collected for an additional 20-min period. DNP-SG and TC biliary excretions were calculated as the product between bile flow and biliary concentration of these compounds, and then referred to basal values. Data are expressed as mean ± S.D. *Significantly different from control. #Significantly different from MDC + E17G ($p < 0.05$; $n = 3$ animals per group).

Figure 7: MDC prevents E17G-induced endocytosis of BSEP and MRP2 in IPL. A. *Representative confocal images of BSEP and MRP2 under the different treatments***.** BSEP (green) and occludin (red) are shown in the upper images, and MRP2 (green) and occludin (red) in the lower ones. In control IPLs, both transporters are circumscribed to the canalicular space, which was delineated by occludin staining. E17G induced a clear internalization of vesicles containing

the transporters beyond the limits of the canaliculi (arrows), and this phenomenon was significantly prevented by a pre-treatment with MDC (100 µM, 15 min prior to E17G bolus, and maintained throughout the perfusion period). MDC *per se* does not produce any change in the location of transporters. **B.** *Densitometric analysis of the fluorescence intensity profile associated with BSEP, MRP2 and occludin.* Densitometric analysis of images was performed along a line perpendicular to the canalicular vacuole (4 µM to each side of the vacuole center), by using ImageJ software. A schematic representation of this procedure is shown (inset), where the canalicular center is represented by a dotted line. The limits of the canalicular space were identified by occludin-associated fluorescence (B, right). Each profile was normalized to the sum of all intensities of the respective measurement. The internalization of transporters induced by E17G resulted in a decrease in the fluorescence intensity associated with the transporters in the canalicular area (flattening of the curve), associated with an increase of it at a greater distance from the canaliculus (widening of the curve). Statistical analysis of the profiles revealed a significant internalization of transporters under E17G treatment ($p < 0.01$ *vs.* control). This internalization was completely abolished by MDC ($p < 0.01$ *vs.* E17G, n = 20-50 canaliculi per preparation, from 3 independent preparations). None of the treatments affected the normal distribution of actin. Data are expressed as mean ± S.E.M.

Figure 8: E17G induced a redistribution of BSEP and MRP2 in raft and non-raft microdomains. Liver samples were taken at time 0 and 20 min after injecting E17G, or its vehicle in controls. Raft and non-raft fractions were obtained from highly purified plasma liver membranes. **A.** Representative western blot for caveolin-1 (raft marker), clathrin (non-raft marker), BSEP and MRP2 on raft and non-raft microdomains. **B.** Distribution of BSEP in rafts and non-rafts. **C.** Distribution of MRP2 in rafts and non-rafts. Data are expressed as mean ± S.D., n = 3 from 3 independent experiments. *p <0.05 *vs.* control (basal and 20 min).

Figure 9: Schematic representation displaying the main findings of this work. BSEP and MRP2, are mainly localized in cholesterol- and caveolin-enriched "raft" microdomains under physiological conditions. Under a cholestatic insult induced by E17G, the transporters would shift from the "raft" to "non-raft" microdomains, where they can be endocytosed via the clathrin-mediated pathway. This process involves interaction of the transporters with the adaptor protein AP2, which triggers clathrin-dependent endocytosis. Endocytosed transporter-containing vesicles traffic to apical early endosomes (AEE), from where they can either traffic to Rab11-positive apical recycling endosomes (ARE) or being sorted to lysosomal and/or proteasomal degradation.

In addition, E17G prevents ARE from trafficking to the apical membrane, so that the transporters are retained in this intracellular compartment.

Highlights

- E17G-induced endocytosis of BSEP/MRP2 depends on clathrin, but not caveolin.
- Knock down of the clathrin adaptor AP2 blocks E17G-induced BSEP/MRP2 endocytosis.
- E17G increases colocalization of BSEP/MRP2 with clathrin, AP2 and Rab5.
- E17G induces a shift of BSEP/MRP2 from raft to non-raft membrane microdomains.

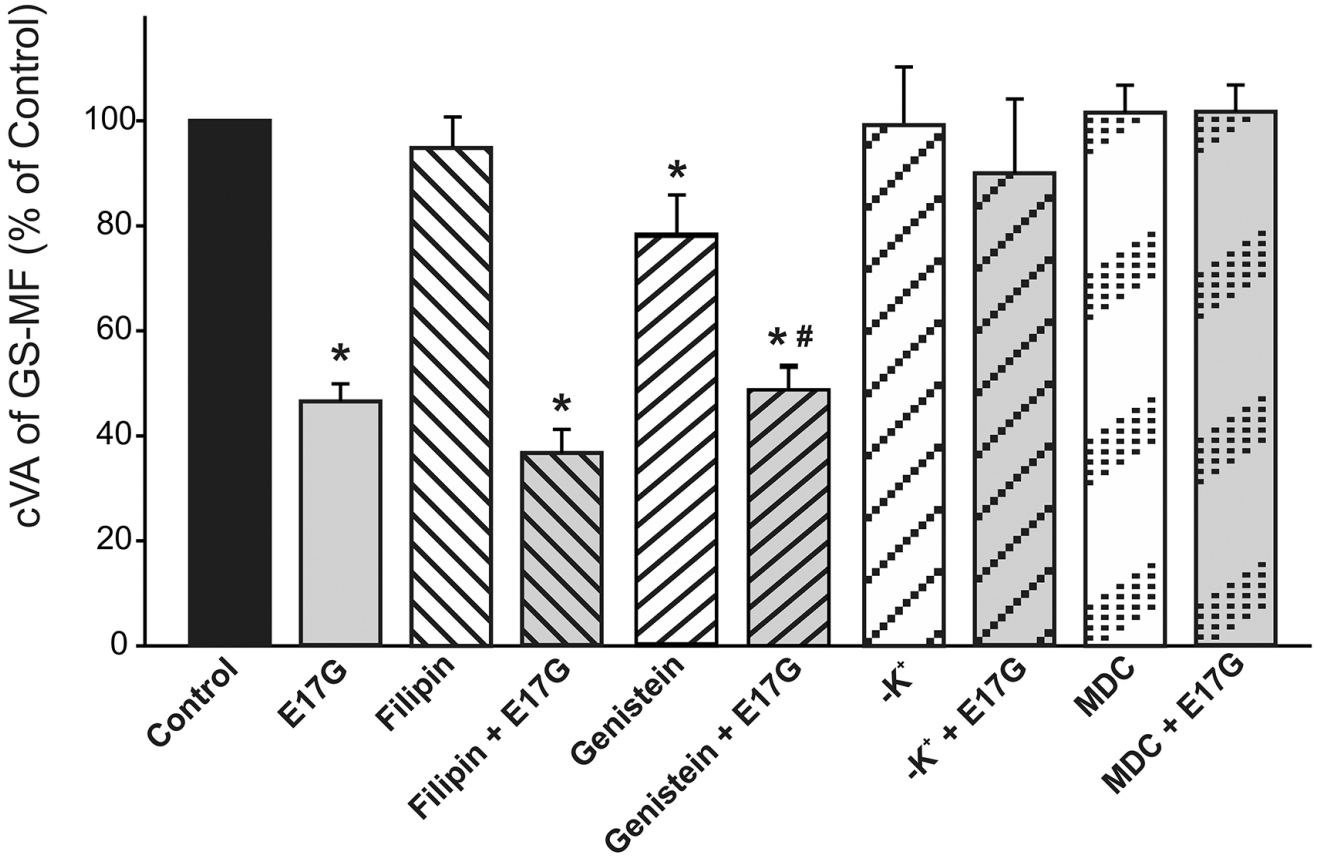
cVA of GS-MF (% of Control)
100
80
60
40
20
0
*
*
*
* #
Control
E17G
Filipin
Filipin + E17G
Genistein
Genistein + E17G
-K+
-K+ + E17G
MDC
MDC + E17G

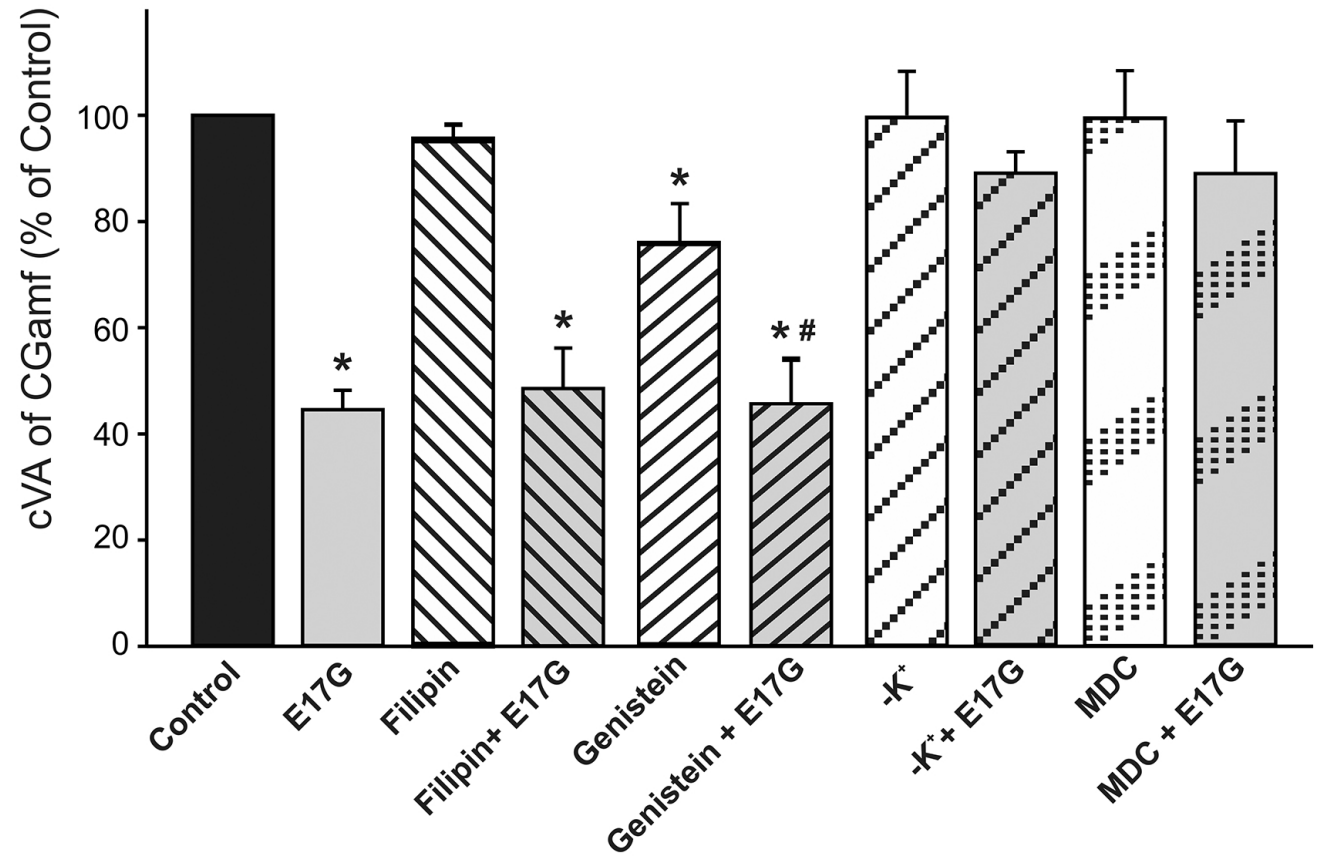
cVA of CGamf (% of Control)
100
80
60
40
20
0
*
*
*
* #
Control
E17G
Filipin
Filipin+ E17G
Genistein
Genistein + E17G
-K+
-K+ + E17G
MDC
MDC + E17G

Figure 1

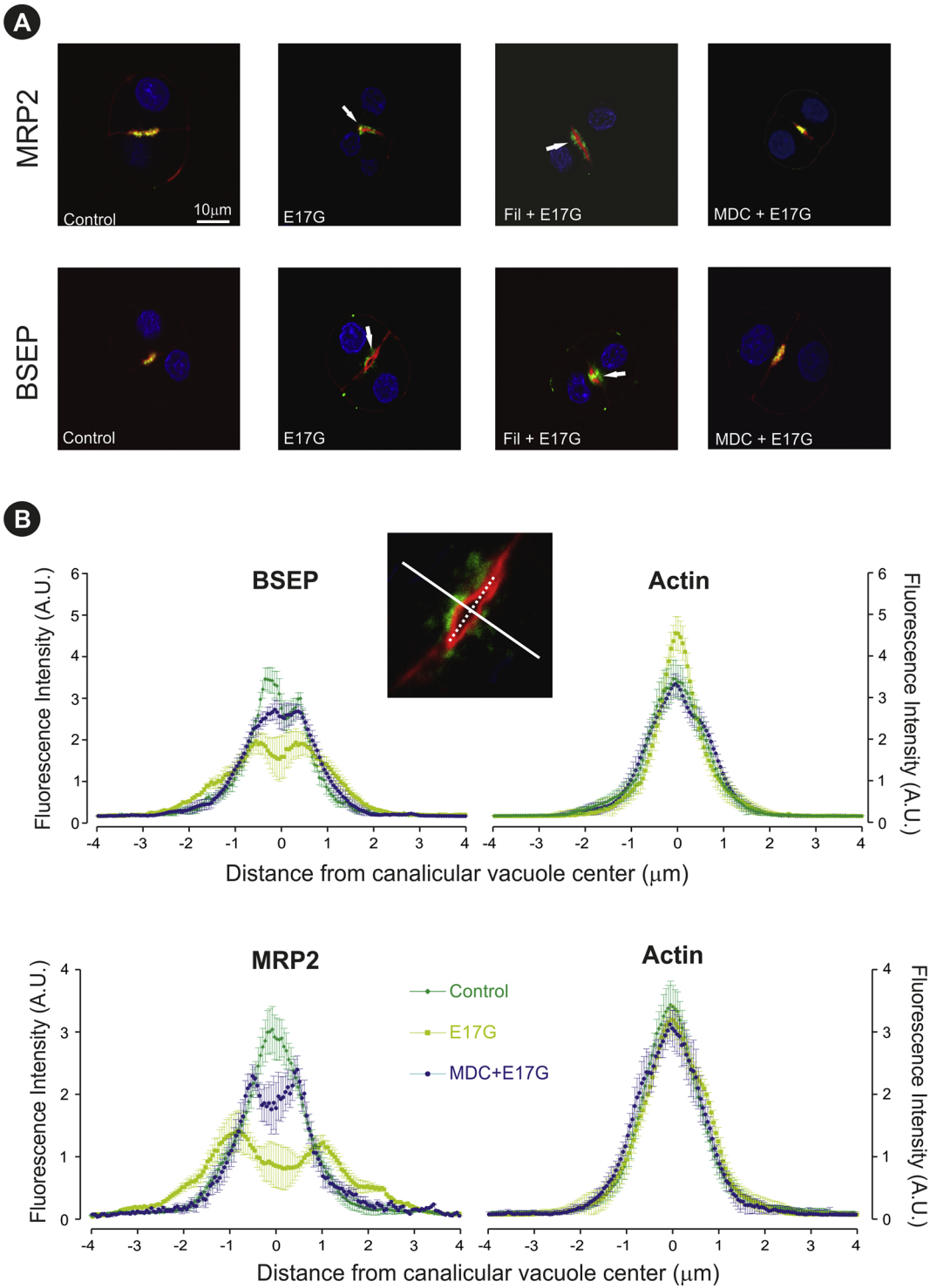
A
MRP2
Control
10μm
E17G
Fil + E17G
MDC + E17G
BSEP
Control
E17G
Fil + E17G
MDC + E17G
B
BSEP
Actin
Fluorescence Intensity (A.U.)
Distance from canalicular vacuole center (μm)
MRP2
Actin
Control
E17G
MDC+E17G
Fluorescence Intensity (A.U.)
Distance from canalicular vacuole center (μm)

Figure 2

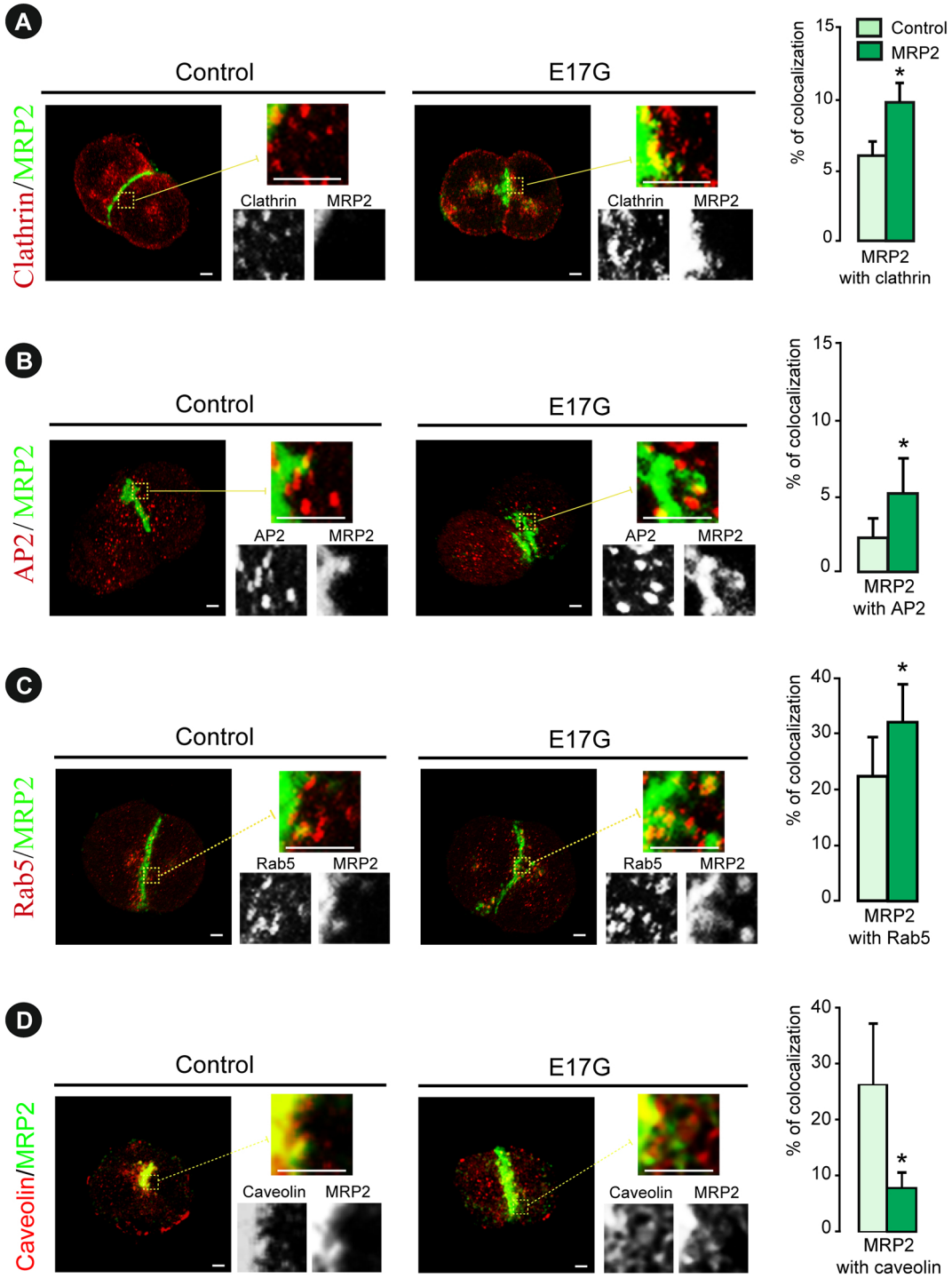
A
Control
E17G
Clathrin/MRP2
Clathrin
MRP2
% of colocalization
Control
MRP2
MRP2
with clathrin
B
AP2/MRP2
AP2
MRP2
MRP2
with AP2
C
Rab5/MRP2
Rab5
MRP2
MRP2
with Rab5
D
Caveolin/MRP2
Caveolin
MRP2
MRP2
with caveolin

Figure 3

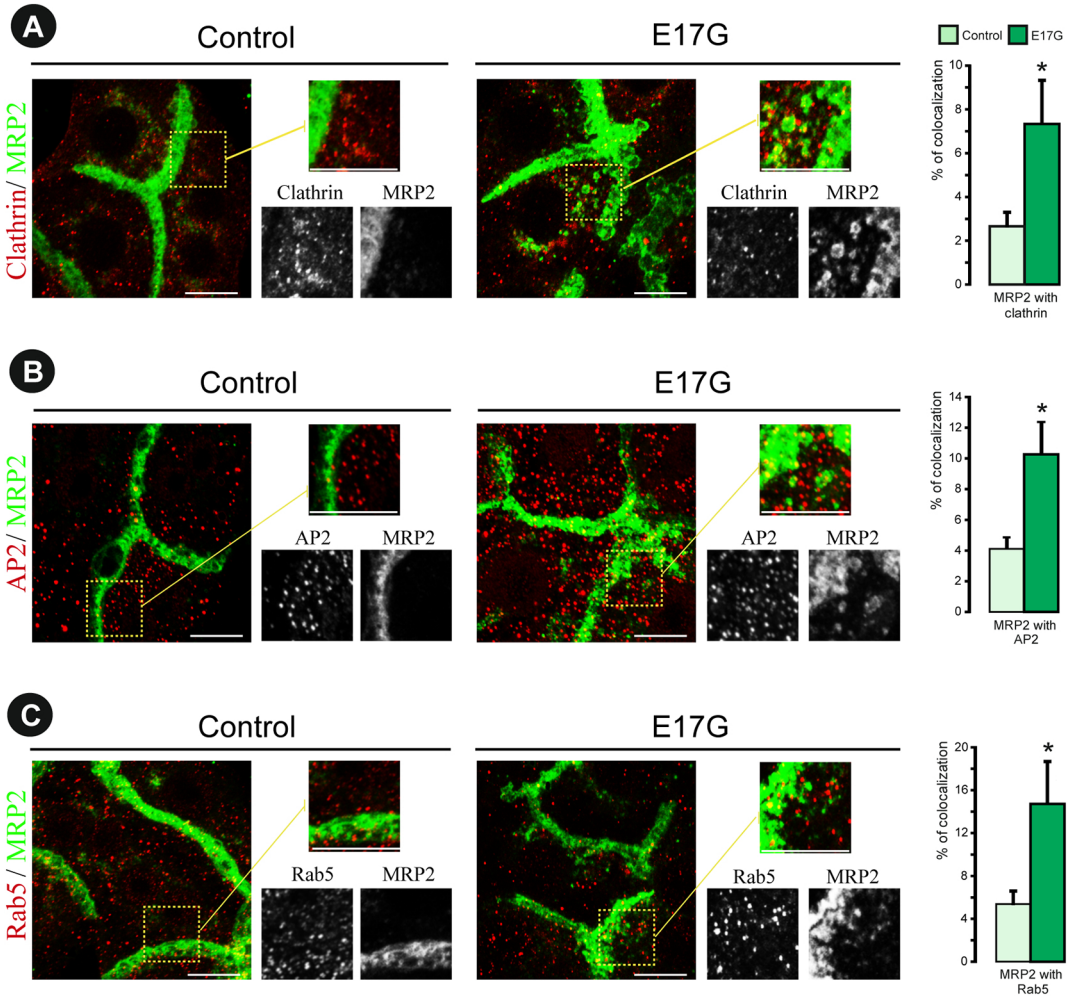
A
Control
E17G
Control
E17G
Clathrin/ MRP2
Clathrin
MRP2
Clathrin
MRP2
% of colocalization
MRP2 with clathrin
B
Control
E17G
AP2/ MRP2
AP2
MRP2
AP2
MRP2
% of colocalization
MRP2 with AP2
C
Control
E17G
Rab5 / MRP2
Rab5
MRP2
Rab5
MRP2
% of colocalization
MRP2 with Rab5

Figure 4

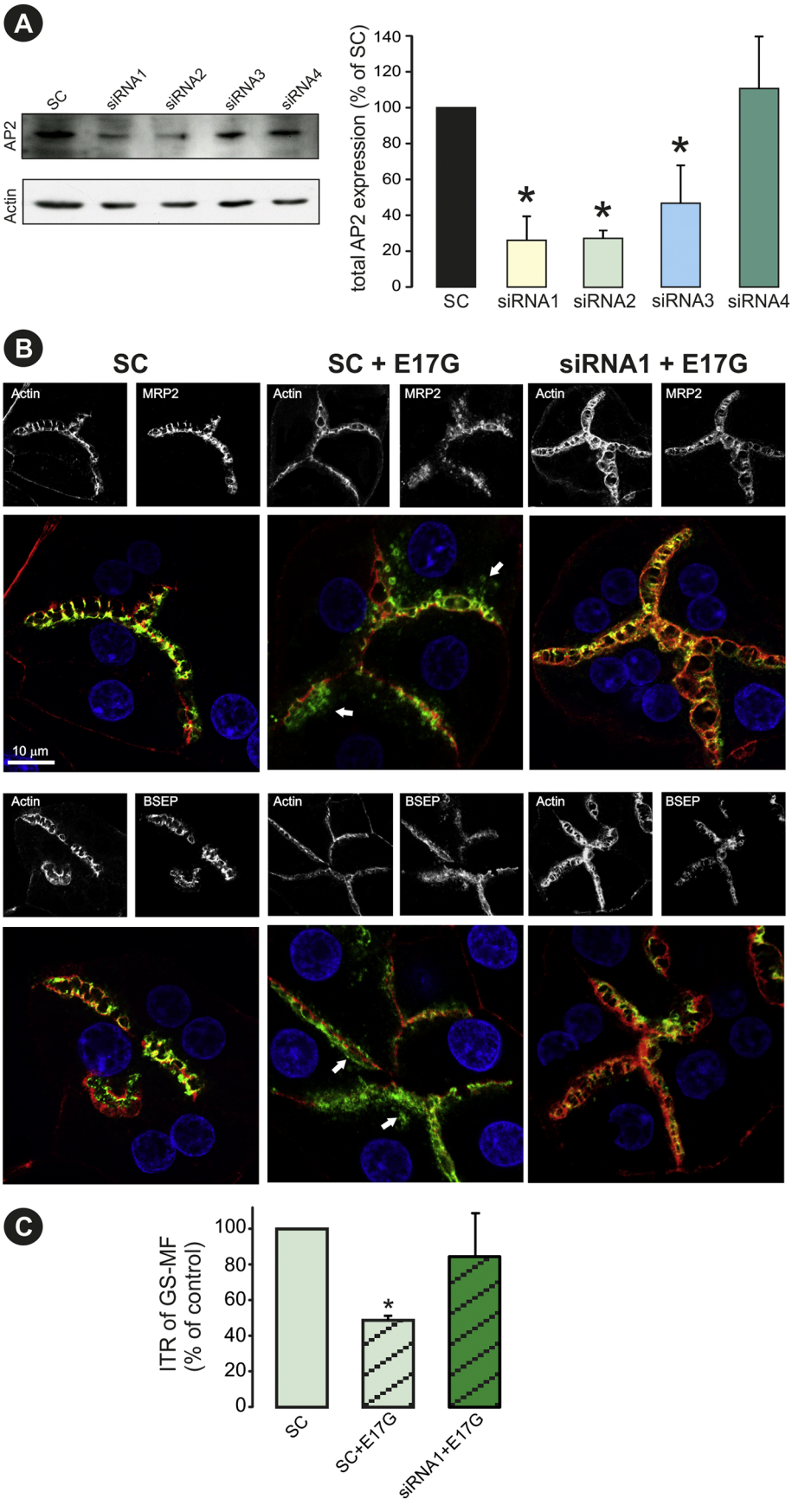
A
SC
siRNA1
siRNA2
siRNA3
siRNA4
AP2
Actin
total AP2 expression (% of SC)
140
120
100
80
60
40
20
0
SC
siRNA1
siRNA2
siRNA3
siRNA4
B
SC
SC + E17G
siRNA1 + E17G
Actin
MRP2
10 µm
BSEP
C
ITR of GS-MF (% of control)
100
80
60
40
20
0
SC
SC+E17G
siRNA1+E17G

Figure 5

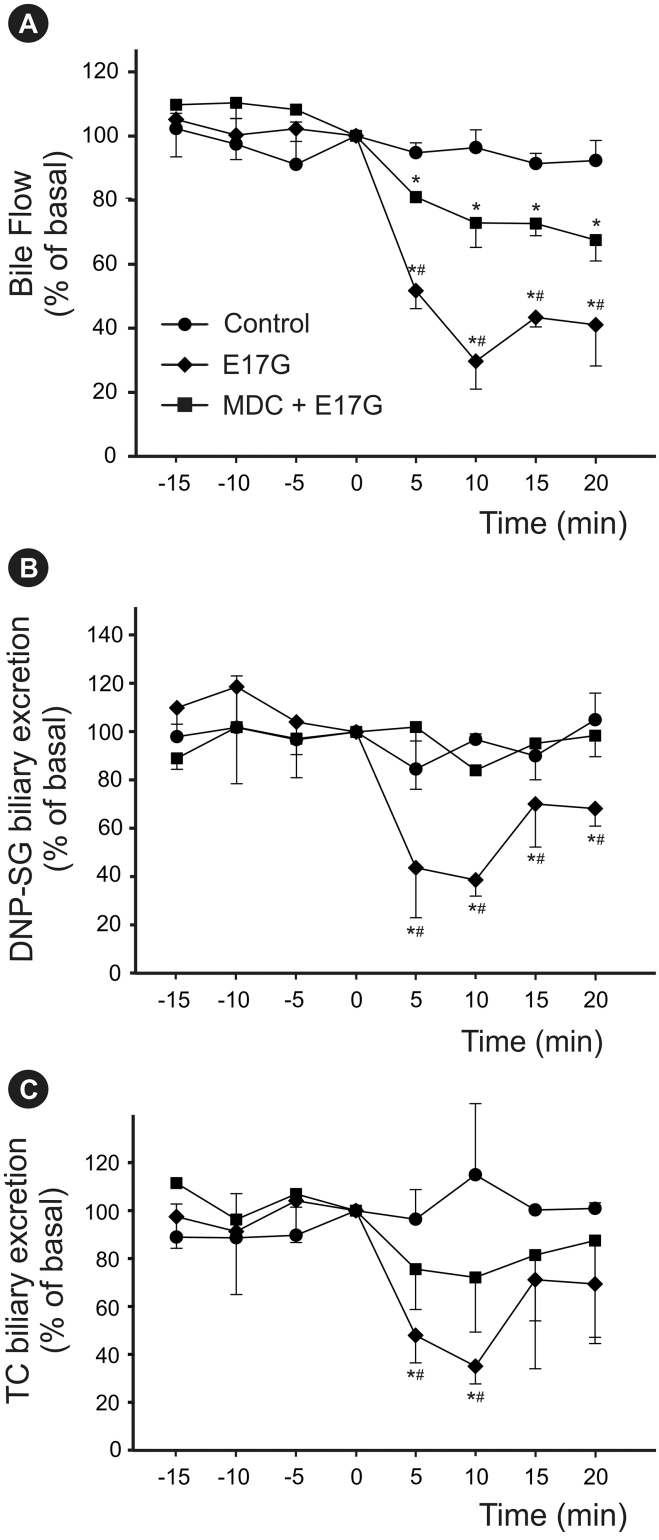
A
Bile Flow
(% of basal)
120
100
80
60
40
20
0
Control
E17G
MDC + E17G
-15
-10
-5
0
5
10
15
20
Time (min)
B
DNP-SG biliary excretion
(% of basal)
140
120
100
80
60
40
20
0
Time (min)
C
TC biliary excretion
(% of basal)
120
100
80
60
40
20
0
Time (min)

Figure 6

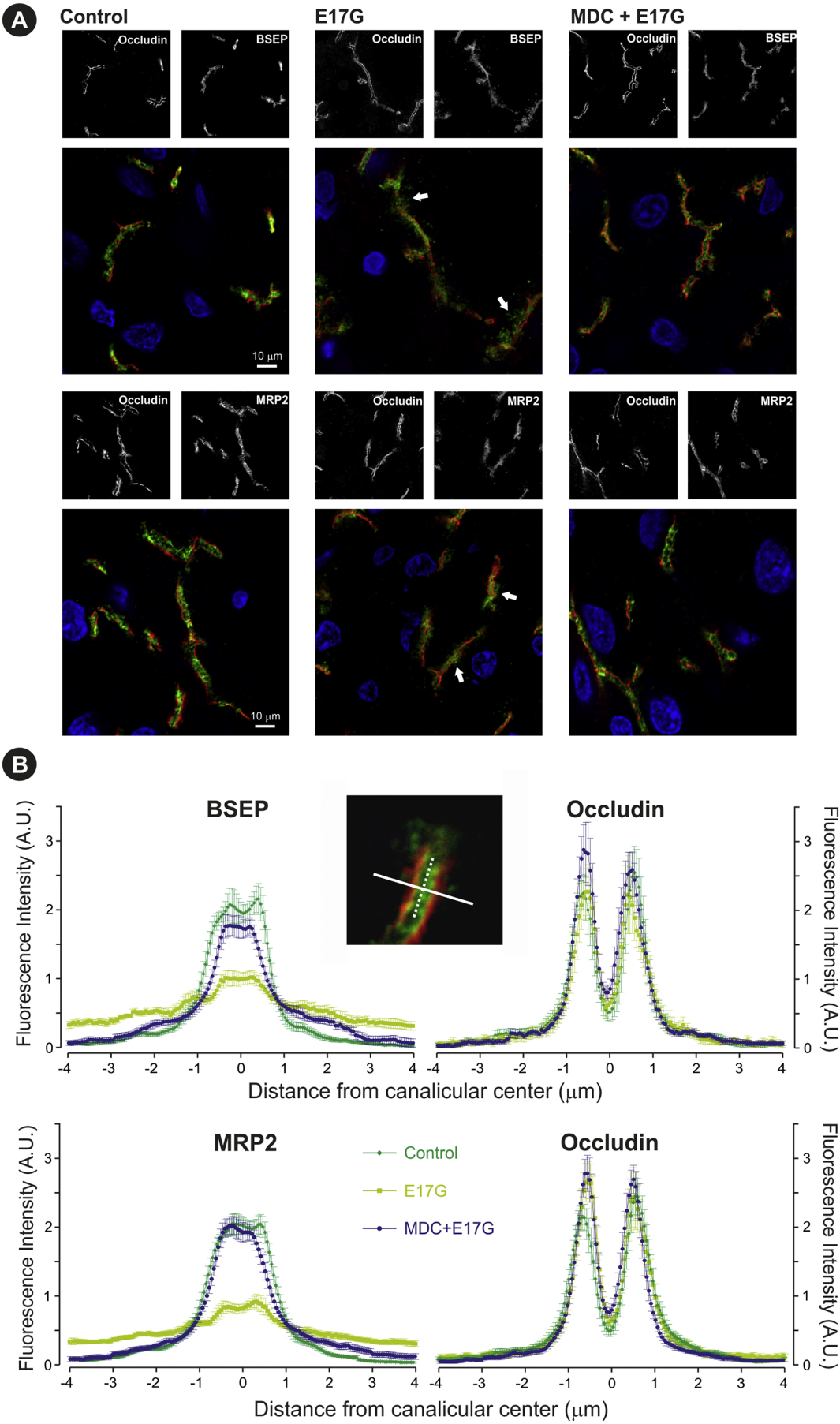
A
Control
E17G
MDC + E17G
Occludin
BSEP
MRP2
10 μm
B
BSEP
Occludin
MRP2
Control
E17G
MDC+E17G
Fluorescence Intensity (A.U.)
Distance from canalicular center (μm)

Figure 7

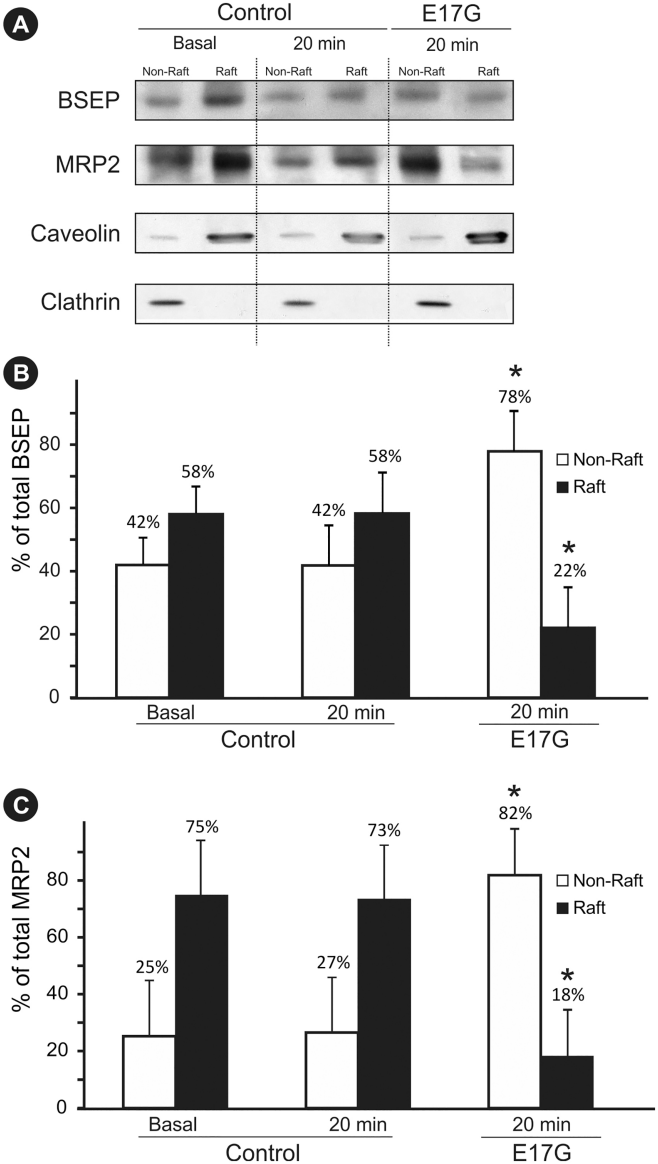
A
Control
E17G
Basal
20 min
20 min
Non-Raft
Raft
Non-Raft
Raft
Non-Raft
Raft
BSEP
MRP2
Caveolin
Clathrin
B
% of total BSEP
0
20
40
60
80
42%
58%
42%
58%
78%
22%
*
*
Non-Raft
Raft
Basal
20 min
20 min
Control
E17G
C
% of total MRP2
0
20
40
60
80
25%
75%
27%
73%
82%
18%
*
*
Non-Raft
Raft
Basal
20 min
20 min
Control
E17G

Figure 8

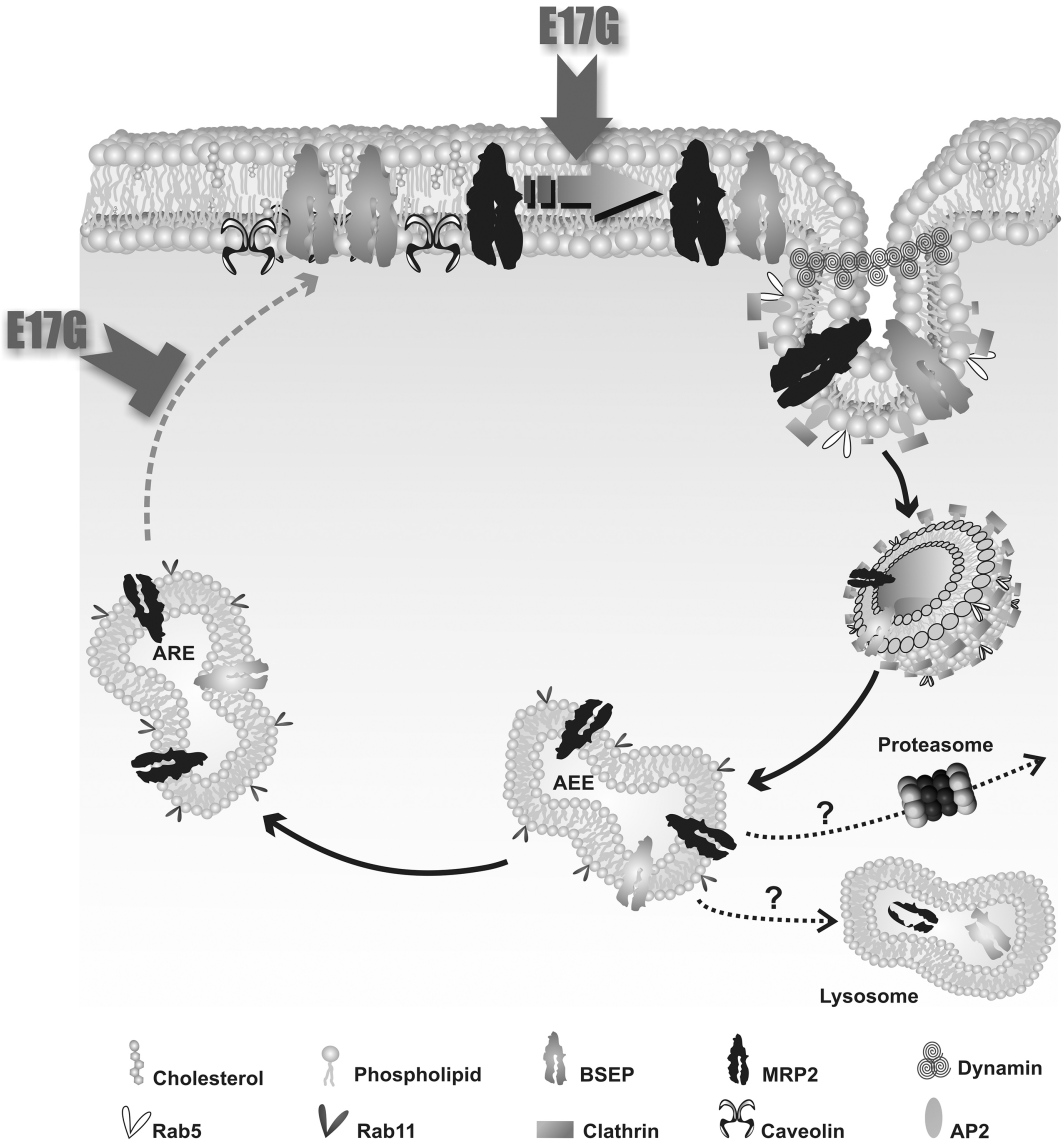
E17G
E17G
ARE
AEE
Proteasome
?
?
Lysosome
Cholesterol
Phospholipid
BSEP
MRP2
Dynamin
Rab5
Rab11
Clathrin
Caveolin
AP2

Figure 9